12

Guided-Mode Resonance Filters Fabricated with Soft Lithography

Kyu J. Lee[1], Jungho Jin[2], Byeong-Soo Bae[2] and Robert Magnusson[1]
[1]*Department of Electrical Engineering, University of Texas at Arlington, Texas*
[2]*Department of Materials Science and Engineering,*
Korea Advanced Institute of Science and Technology, Daejeon
[1]*USA*
[2]*Republic of Korea*

1. Introduction

Methods of microscale and nanoscale patterning can be applied to fabricate a variety of optical devices. Periodic layered structures are found in integrated optics, communication systems, spectroscopy, lasers, and in many other important optical systems. Diffractive optical elements and photonic crystals consist of fine periodic patterns affecting the spectrum, polarization, phase, and amplitude of light. Often, holographic interferometry, or direct electron-beam patterning, is used to define the periodic structure. As an alternative method, soft lithography is effective for fabricating and transferring periodic patterns and structures as reported in recent papers (Xia & Whitesides, 1998) (Xia et al., 1999) (Schmid & Michel, 2000) (Odom et al., 2002) (T.-W. Lee et al., 2005) (Tang et al., 2003) (Rogers & Nuzzo, 2005) (D.-H. Lee et al., 2007). Accordingly, using methods and processes associated with soft lithography, new narrow-band resonant optical filters fabricated in hybrimer compounds are presented.

In this work, a new material system for fabricating the resonant optical filters is employed. Hybrimers are typical organic-inorganic hybrid materials fabricated using a sol-gel process (Choi et al., 2005) (Kim et al., 2006) (Kim et al., 2005). Hybrimers have several advantageous properties, including high modulus, low surface tension, low shrinkage, and high etching resistance. In particular, they have excellent optical properties including high transparency (>90% in the visible region), controllable refractive indices, low optical loss (<0.2 dB/cm), low birefringence (~10^{-4}), and low viscosity compared to common ultraviolet (UV)-curable polymers (Kim et al., 2005) (T.-H. Lee et al., 2006). These materials possess thermal stability beyond 300 ^{o}C. The versatile properties of hybrimers offer new options for practical applications related to micro-optical devices. In the case of the fluorinated hybrimer used in this work, an organoalkoxysilane precursor functionalized with a perfluoroalkyl chain is used in the sol-gel reaction to lower the surface tension of the final compound. Hybrimers qualify both as molds and as resists in nanoimprint lithography (Kim et al., 2006). Significantly, there is no additional chemical treatment needed to release the mold due to the presence of fluorine molecules in the hybrimer compound.

We present guided-mode resonance (GMR) filters fabricated by soft lithography with hybrimer materials. The term GMR refers to a rapid variation in the intensities of the electromagnetic fields in a periodic waveguide, or photonic crystal slab, as the wavelength or the angle of incidence of the excitation light varies around their resonance values. A resonance occurs when incident light is phase-matched to a leaky guided mode allowed by the waveguide-grating structure (Magnusson & Wang, 1992). Numerous potentially useful devices based on resonant waveguide modes have been theoretically predicted and experimentally verified (Magnusson & Wang, 1992) (Avrutsky & Sychugov, 1989) (Peng & Morris, 1996) (Ding & Magnusson, 2004) (K.J. Lee & Magnusson, 2011)(Sharon et al., 1996) (Brundrett et al., 1998) (Priambodo et al., 2003) (Liu et al., 1998) (K.J. Lee et al., 2008). However, these devices were designed to work with conventional materials and processes. Therefore, additionally, we provide example fabrication and characterization of GMR filters made by soft lithography. As these resonant elements are highly sensitive to parametric variations, it is important to develop methods for their reliable fabrication. Thus, we provide a fabrication process that is consistent and simple, employing an elastomeric mold and a UV-curable organic-inorganic hybrid material. A particular fabricated device exhibits measured spectra showing ~81% reflectance and ~8% transmittance at a resonance wavelength of 1538 nm. The filter's linewidth is ~4.5 nm, and the sideband reflectance is ~5%. Experimental and theoretical results are in good agreement. We conclude that soft lithography combined with hybrimer media is an advantageous methodology for fabricating resonant photonic devices.

2. Fabrication of a surface-relief structure with optical polymers

Before hybrimers were considered UV-curable materials for surface-relief structures, commercially available optical prepolymers such as J-91, SK-9 (Summers Optical), and NOA-73 (Norland Products Inc.) were applied in soft lithography. Table 1 shows the main properties of these materials (Summers) (Norland).

Product name	Material	Refractive index	Viscosity (cps)
J-91	polyurethane	1.55	250 ~ 300
SK-9	polyacrylate	1.49	80 ~ 100
NOA-73	polyurethane	1.56	130

Table 1. The properties of three commercial optical prepolymers

2.1 Fabrication process of GMR filters by microtransfer molding

Soft lithography uses soft elastomeric materials to make patterns and structures without the use of complicated and expensive facilities that conventional photolithography uses. Therefore, soft lithography has been shown to be a simple and cost-effective method for pattern transfer. Xia and Whitesides reported several soft lithography methods including replica molding (REM), microtransfer molding (μTM), micromolding in capillaries (MIMIC), and solvent-assisted micromolding (SAMIM) (Xia & Whitesides, 1998). Of the four methods, we choose to conduct preliminary fabrication using the μTM method. REM duplicates the structure with a thick supporting layer, which is not desired for GMR device implementation. MIMIC requires very low-viscosity materials and it cannot get capillary filling with the optical prepolymers in Table 1. SAMIM is a method which applies a solvent that can dissolve or soften the material to form the structure. It is also not proper for our application.

Fig. 1 summarizes the procedure for fabrication of the GMR device using a μTM method. The first step of the fabrication is making a master template, which has the requisite grating structure on the surface of a silicon wafer. The silicon grating structure can be made by photoresist spin-coating, holographic recording, photoresist development, and plasma etching. These conventional fabrication process steps using photolithography are described, for example, in (Priambodo et al., 2003). However, for the results reported here, two types of commercial holographic gratings (Newport Co.) are used as master templates. One has 556 nm grating period (1800 grooves/mm) and ~170 nm grating depth for developing GMR devices operating in the near-infrared region (~850 nm wavelength). Another grating has 1111-nm grating period (900 grooves/mm) and ~340 nm grating depth for the communication band (~1550 nm wavelength). These gratings have sinusoidal profiles.

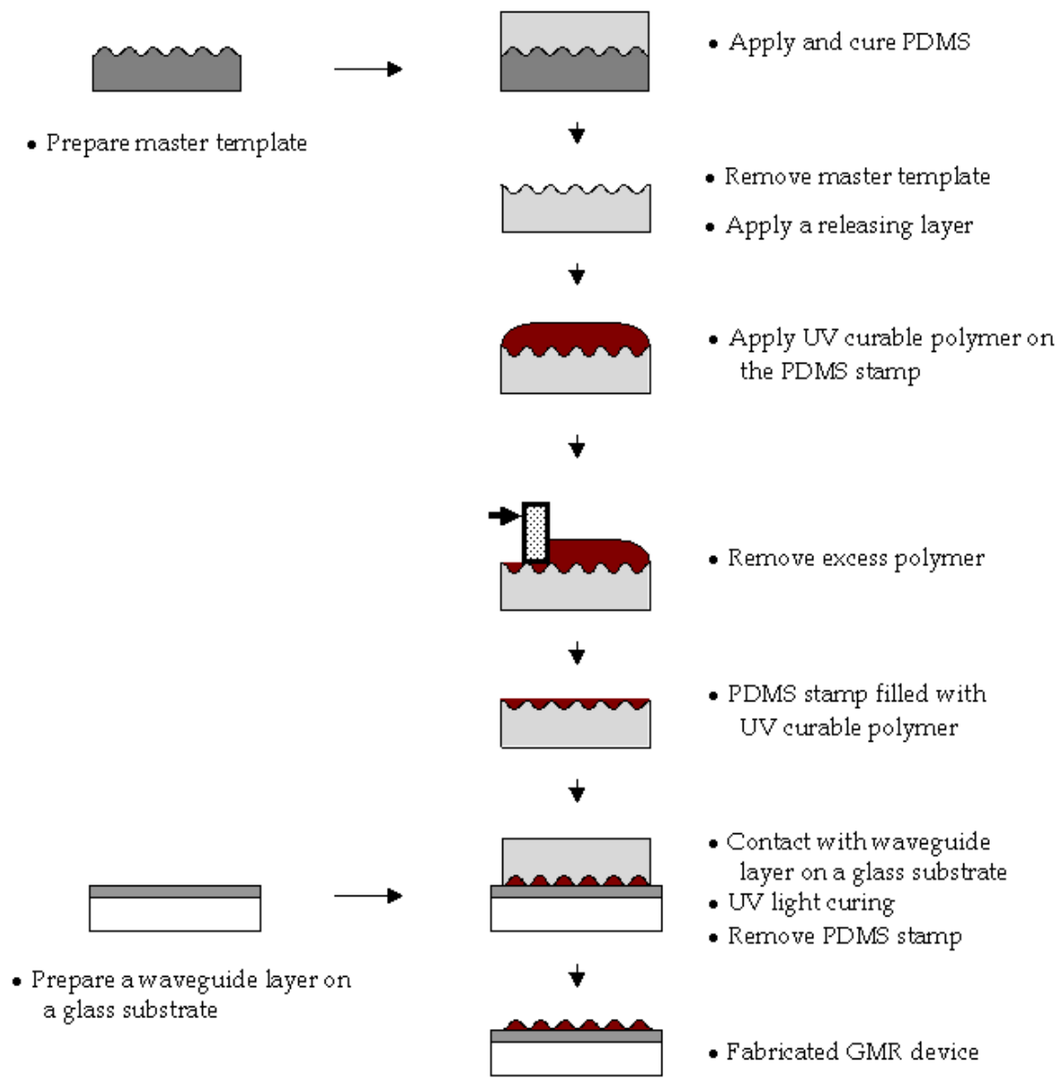

Fig. 1. Schematic fabrication process of a GMR device by μTM

As an elastomeric mold, polydimethylsiloxane (PDMS) is commonly used in soft lithography. Sylgard 184 silicone elastomer from Dow Corning, which is commonly used, is applied. Sylgard 184 silicone elastomer is mixed in a 10:1 ratio of base and curing agent and its mixture is degassed in a vacuum to eliminate bubbles. The prepolymer of Sylgard 184 is poured onto the top of the master template and cured at room temperature for 48 hours. The result is a mold with the negative replica of the grating on its surface. Atomic force microscope (AFM) images of the master template and the replica are shown in Fig. 2. These AFM images are obtained by Asylum MFP-3D AFM (Asylum Research).

A few drops of a UV-curable optical prepolymer are applied on the patterned surface of the elastomeric mold. The excess prepolymer is scraped off using a flat PDMS block, such that the grooves of the PDMS mold are filled with UV-curable prepolymer. Next, the filled PDMS mold is put in contact with a silicon nitride (Si_3N_4) thin-film on a glass substrate. As a waveguide layer, the Si_3N_4 thin-film is prepared by sputtering; this layer can also be replaced by a high-refractive index polymer material, such as a titanium dioxide (TiO_2)-rich film made by spin-coating (Wang et al., 2005). The prepolymer is cured using a UV lamp (central wavelength λ = 365 nm). Patterned grating structures are obtained on the Si_3N_4 film after the PDMS mold is peeled off.

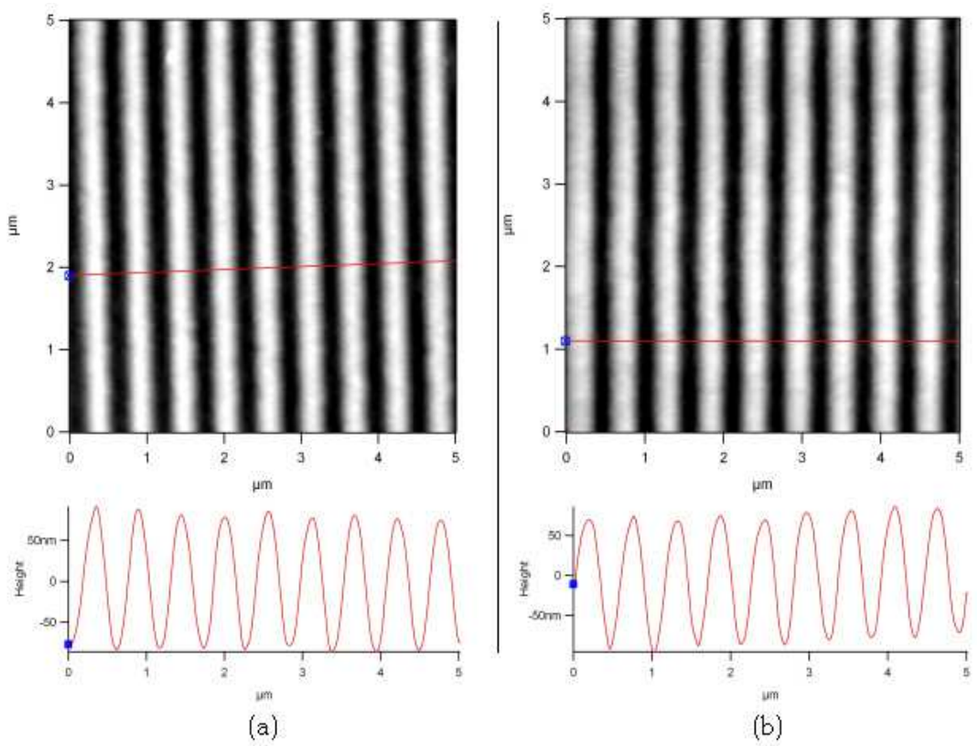

Fig. 2. AFM images of (a) the master template and (b) the replica. The size of the scanned area is 5 µm x 5 µm

2.2 Discussion of the fabrication process

Fig. 2 shows AFM images of the master template and the PDMS stamp. Both images show approximately sinusoidal profiles and a grating period of 556 nm. The average depths of

the grating layer for the master template and the PDMS stamp are ~170 nm and ~168 nm, respectively. Odom et al. demonstrated that soft lithography techniques are useful for the patterning on the size scale of 500 nm and larger. However, the application of these methods is limited in the sub-100-nm range because of the low modulus (2.0 N/mm^2) of PDMS (Odom et al., 2002). During the process, deformations such as roof collapse and lateral collapse can occur in the PDMS stamp and details of deformations are discussed in (Schmid & Michel, 2000) (Odom et al., 2002) (T.-W. Lee et al., 2005). This deformation is also found in our processes reported here. For example, Fig. 3 shows AFM images of the deformed area. This deformation is more evident if there are higher aspect ratios. Fig. 4 shows AFM images of a PDMS stamp having a 520-nm grating period and 220-nm grating depth, which is prepared by photoresist grating. Pairings of grating lines are easily observed in this image. Delamarche et al. discussed the stability of lines molded in PDMS with different mold thicknesses and showed the limitation of shape formation in PDMS without deformation (Delamarche et al., 1997). They also proposed that surface treatment with 1% sodium dodecylsulfate in water and a heptane rinse could provide the recuperation of the paired lines. Even though their method is applied to this stamp, it shows little improvement.

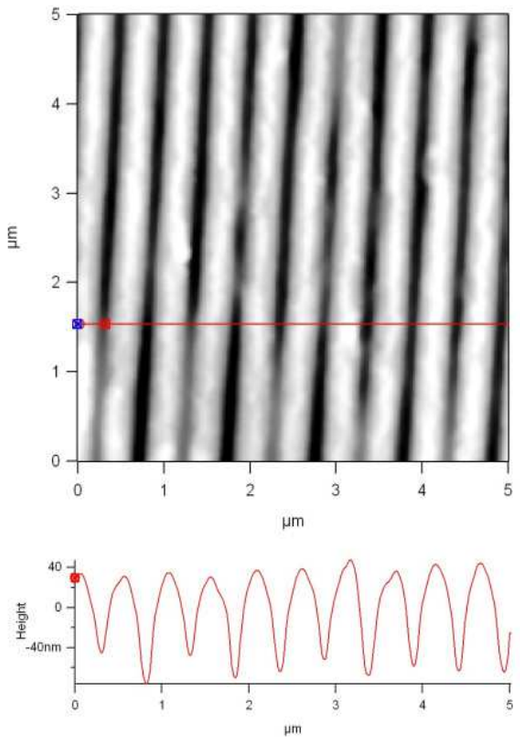

Fig. 3. AFM image of a deformed area on a PDMS stamp. The size of the scanned area is 5 µm x 5 µm

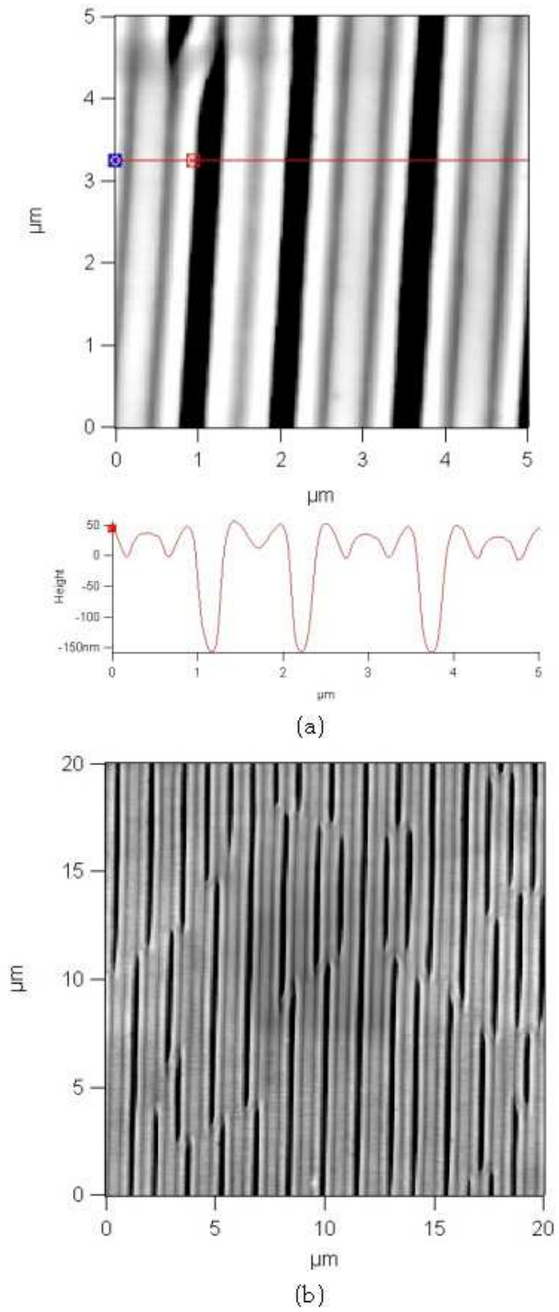

Fig. 4. AFM images of a PDMS stamp having a 520-nm grating period and 220-nm grating depth showing grating-line pairing. The size of the scanned areas are (a) 5 µm × 5 µm and (b) 20 µm × 20 µm

Schmid et al. formulated an alternative siloxane polymer, called hard-PDMS (h-PDMS), which has a higher modulus (~9 N/mm^2) than that of Sylgard 184 silicone elastomer (Schmid & Michel, 2000) (Odom et al., 2002). Odom et al. and Lee et al. demonstrated improved results of surface structure formation by using h-PDMS compared with Sylgard 184 PDMS (Odom et al., 2002) (T.-W. Lee et al., 2005). In our research, we apply h-PDMS as described in Section 3.

In addition, the UV-curable polymers can stick to the PDMS stamp and this causes deformation of the structure during the process. To solve this problem, silane treatment is widely used for the surface of the PDMS stamp and acts as a releasing layer. Tang et al. reported that the modification of PDMS stamps by an adsorbed monolayer of bovine serum albumin (BSA) can provide distortion-free separation between the PDMS stamp and molded gel from the stamp (Tang et al., 2003). In our process, we find that the cured polymer does not attach well to the waveguide but tends to remain on the PDMS stamp after separation. Therefore, we apply the BSA treatment to improve the release. The PDMS stamp is immersed in a 3% solution of aminopropyldimethylethoxysilane (Gelest, SIA0603.0) in methanol for 2 hours. The modified PDMS is next rinsed in phosphate buffer saline (PBS, Fisher Scientific, BP2438-4) solution for 90 seconds. A solution of BSA (100 mg/ml Fisher Scientific, NC9806065) is applied over the patterned surface of the PDMS for 60 seconds. The treated PDMS is then rinsed in a PBS solution for 90 seconds to remove any unbounded BSA. After this BSA treatment, it is possible to successfully get the structure to adhere to the waveguide layer with no remaining polymer in the PDMS stamp.

2.3 Fabrication results

Fig. 5 shows the experimental spectral response of a fabricated GMR device using the NOA-73 prepolymer. A tunable Ti:Sapphire laser pumped by an Argon-ion laser is used to measure its spectral response. The resonance wavelength (maximum point of reflectance) is at λ = 863.6 nm and the full-width at half-maximum (FWHM) linewidth is 4.0 nm. The reflectance at resonance is about 33%. This relatively low efficiency is attributed to the loss of the Si_3N_4 thin-film (measured extinction coefficient, k ~ 10^{-3}) and imperfections on the grating surface. Even though the efficiency of the fabricated device is low, it can be used in resonant sensor devices because high-efficiency is not essential in GMR sensor application and the key quantity is the resonance wavelength shift. Fig. 6 shows AFM images of the GMR device fabricated with NOA-73. The cross-sectional view shows that the thickness of the grating layer is not uniform. This thickness non-uniformity is due to the scraping process applied to remove excess prepolymer by hand.

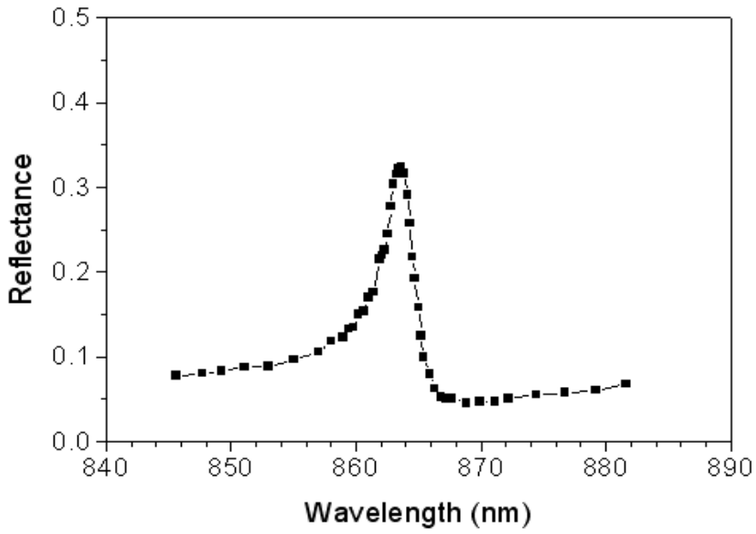

Fig. 5. Experimental spectral response of a fabricated GMR filter for transverse-electric (TE) polarization

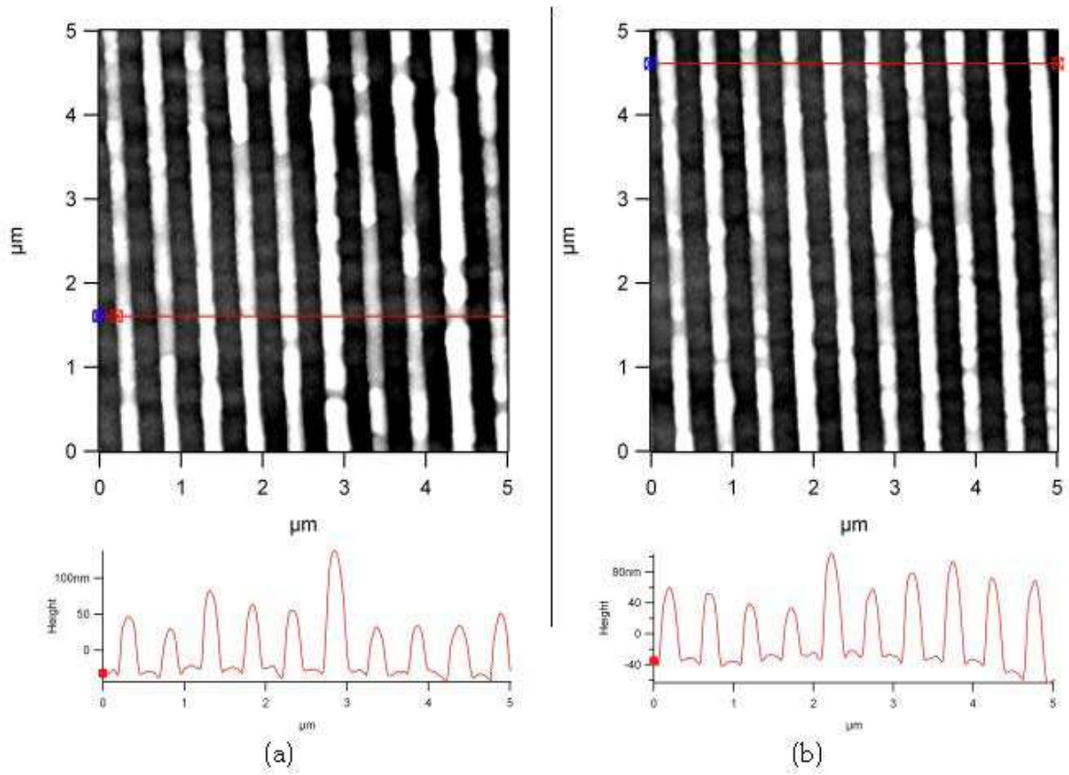

Fig. 6. AFM images of fabricated GMR devices with NOA-73 at two different locations. The size of the scanned area is 5 μm × 5 μm

The structure of GMR filters fabricated by J-91 and SK-9 is not much different from that of the NOA-73 filter as shown in Fig. 6. The improved μTM method with a machine-controlled system was reported by (J.-H. Lee et al., 2005). They used a dragging speed of ~30 μm/sec and a metal blade, which was controlled by mechanical actuators for scraping.

3. Improved fabrication of GMR filters using hybrimers and MIMIC

As described in section 1, hybrimers have many advantages, especially low viscosity, which can be lowered to ~8 cps. This low-viscosity material is applied with the MIMIC method. The combination of hybrimers and MIMIC to fabricate GMR filters is described in this section. It is shown to provide much-improved GMR devices relative to the devices reported above.

3.1 Fabrication process and characterization

Fig. 7 shows a schematic procedure for fabrication of a GMR device using the MIMIC method. As described in section 2.1, MIMIC is one of several soft lithography methods proposed by Whitesides and co-workers, and it is simple to apply (Xia & Whitesides, 1998) (Xia et al., 1999). The first step of the fabrication is preparing a master template, which has the grating structure on the surface of a silicon wafer or a glass substrate. In this section, a commercial holographic grating, which has a 1111-nm grating period and ~340-nm grating depth with a sinusoidal profile is used as a master template.

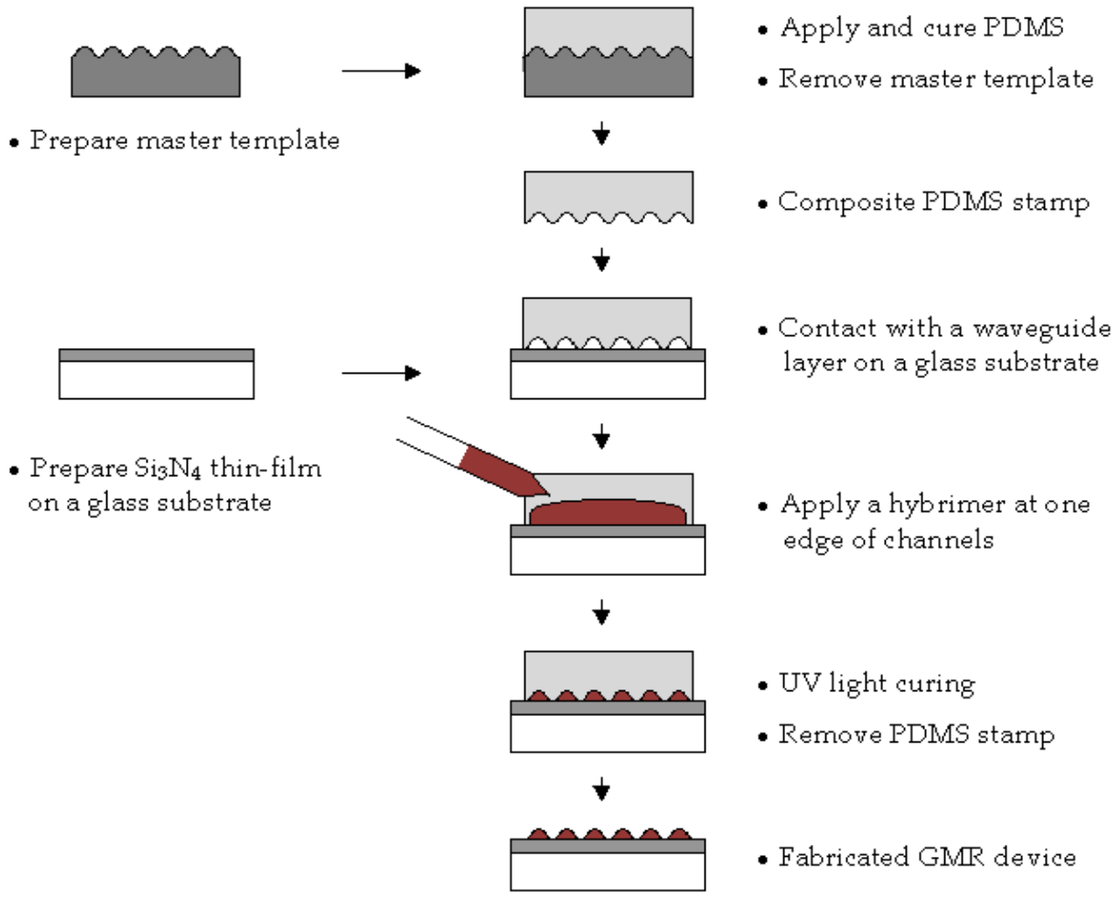

Fig. 7. Schematic fabrication process of a GMR device using the MIMIC method

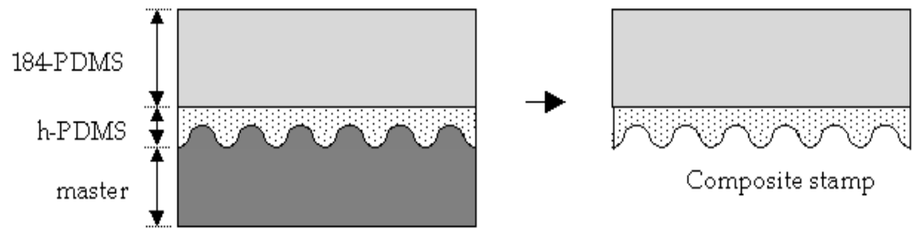

Fig. 8. Configuration of the composite stamp. The h-PDMS is spin-coated on the master template followed by pouring Sylgard 184 PDMS

Composite polymeric stamps as elastomeric molds are applied to achieve high-quality patterning. The composite stamps consist of two parts as shown in Fig. 8; one part is h-PDMS, which has different mechanical properties than the Sylgard 184 silicone elastomer. The other part is Sylgard 184 PDMS to support h-PDMS and maintain the flexibility of the stamp. The h-PDMS is prepared as follows (Odom et al., 2002): a vinyl PDMS prepolymer (3.4 gram, Gelest Inc., VDT-731), platinum (Pt) catalyst (18 µL, Gelest Inc., SIP6831.1), and modulator (50 µL, Sigma-Aldrich, Product No. 87927) are mixed and degassed in a vacuum for 5 minutes. A hydrosilane prepolymer (1.0 gram, Gelest Inc., HMS-301) is added into the mixture and stirred gently to avoid bubbles. Within 5 minutes after stirring, this h-PDMS prepolymer is spin-coated (1000 rpm, 40 sec.) on a commercial holographic grating and cured in an oven at 60 °C for 30 minutes. Then a prepolymer of Sylgard 184 silicon elastomer is poured on the h-PDMS layer and is cured in an oven again at 60 °C for 3 hours. Therefore, a pattern with a negative replica of the master template is formed on the h-PDMS surface. AFM images of the surface of the master template and the composite stamp are shown in Fig. 9. We obtain faithful replication and a high-quality, scatter-free surface.

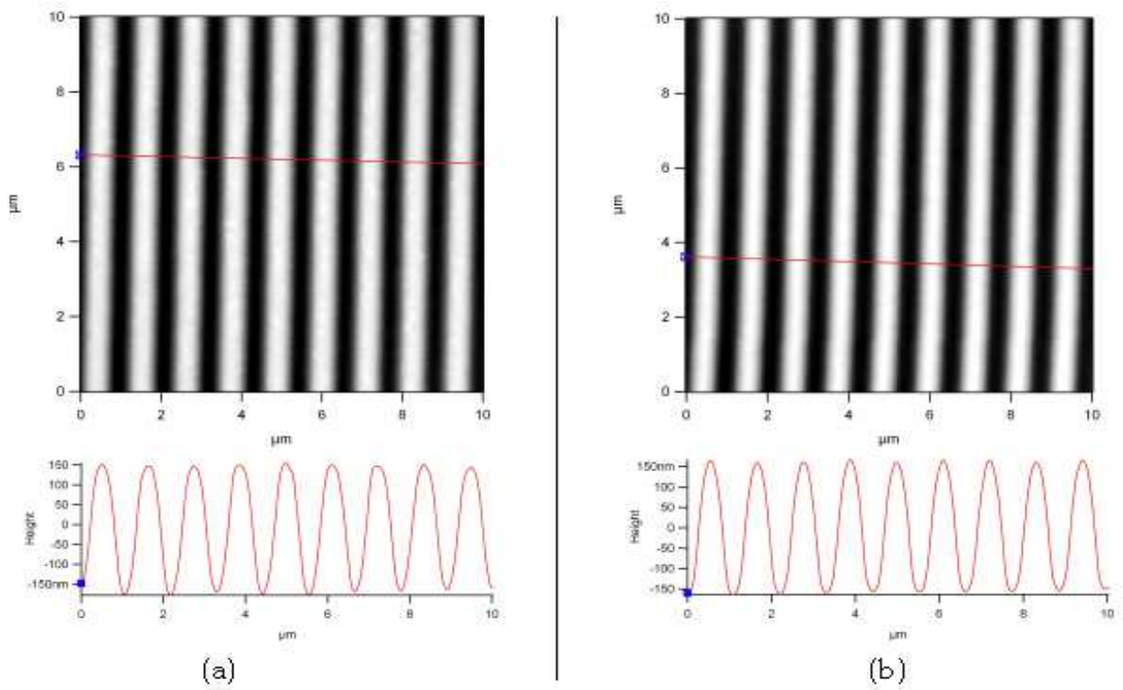

Fig. 9. AFM images of (a) the master template and (b) the composite stamp replica. The size of the scanned area is 10 µm × 10 µm

To realize a GMR filter, the 10mm × 10mm composite mold is placed in contact with a Si_3N_4 thin film on a glass substrate. The Si_3N_4 film, prepared by plasma-enhanced chemical vapor deposition (PECVD, Surface Technology Systems), serves as the waveguide layer of the GMR device. A diluted hybrimer is prepared to obtain a lower viscosity prepolymer. A few drops of the UV-curable hybrimer are applied at one edge of the patterned surface of the composite mold as indicated in Fig. 7. The applied hybrimer spreads through the channels, which are formed by contact between the patterned mold and the thin-film layer on the substrate. Then the composite mold set is put into a vacuum chamber and is allowed to remain in low vacuum (~450 Torr) for 12 hours so that the channels fill with the hybrimer prepolymer by capillary force. Subsequently, the hybrimer in the h-PDMS channel is cured using a UV lamp (central wavelength λ = 365 nm). The surface-relief type grating structure remains on the Si_3N_4 film after the composite mold is peeled off. This easy-release process is associated with the hybrimers medium.

A tunable laser source (HP 8168F) is used to measure the spectral response. The angle of incidence (θ_{in}) is set at 10° to locate the resonance wavelength of the GMR device within the operating spectral range of the laser source. Next, the reflected and transmitted power are measured in the wavelength range of 1450 nm to 1590 nm, in 0.5 nm steps. A polarizer is used to set the polarization state.

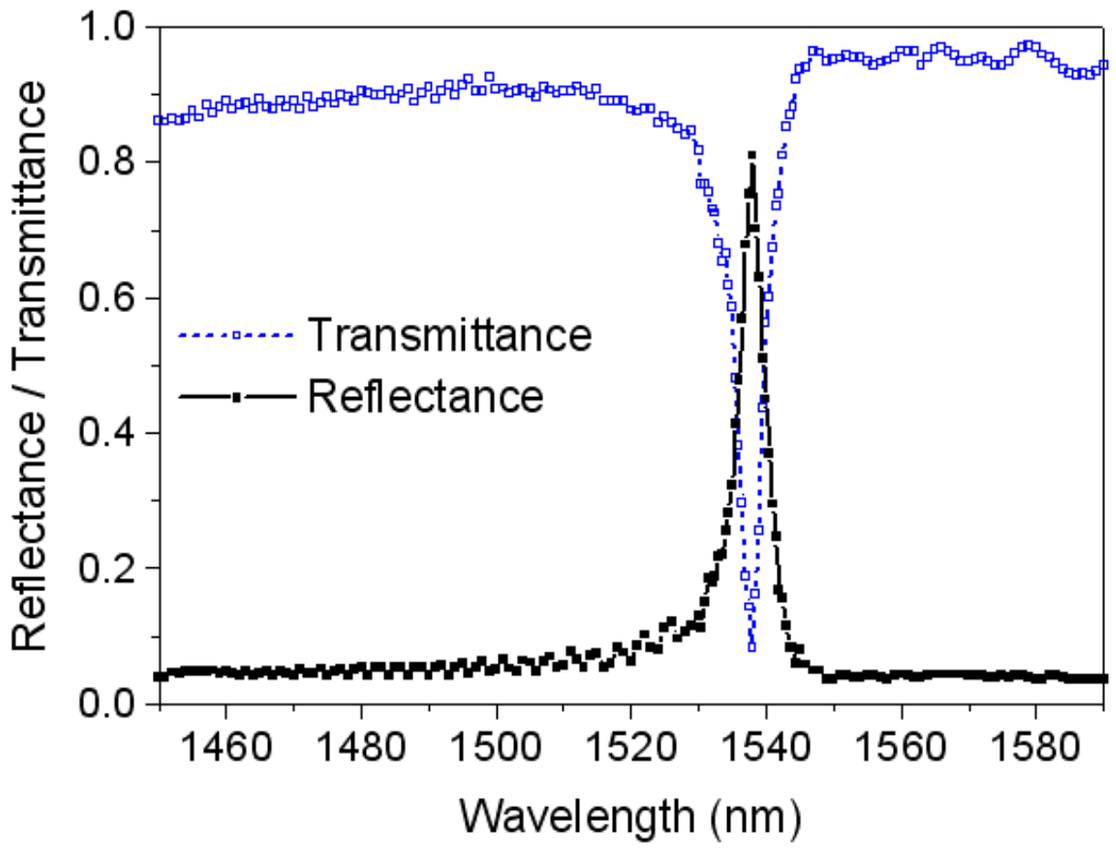

Fig. 10. Experimental spectral response of a fabricated GMR filter for TE polarization

3.2 Results and discussion

Fig. 10 shows the experimental spectral response of the fabricated device. The resonance wavelength (maximum point of reflectance or minimum point of transmittance) is λ = 1538 nm, and the reflectance at resonance is ~81%. The FWHM linewidth is ~4.5 nm, and the sideband reflectance is ~5%. The transmittance at resonance is ~8%. These results pertain to the TE polarization state of the input light.

Fig. 11 shows the calculated spectral response of the fabricated GMR device whose model is shown as an inset. The calculations are performed with a computer code that we wrote based on rigorous coupled-wave theory (Gaylord & Moharam, 1985). The device parameters used in Fig. 11 correspond to the experimental values used in the fabrication. The calculated resonance wavelength is λ = 1536 nm at θ_{in} = 10.0°, and the FWHM linewidth is 4.4 nm. The calculated reflectance at resonance is ~82%. This non-100% reflection is due to the presence of a higher-order transmitted wave at resonance as shown in Fig. 11 and noted as T_{+1}.

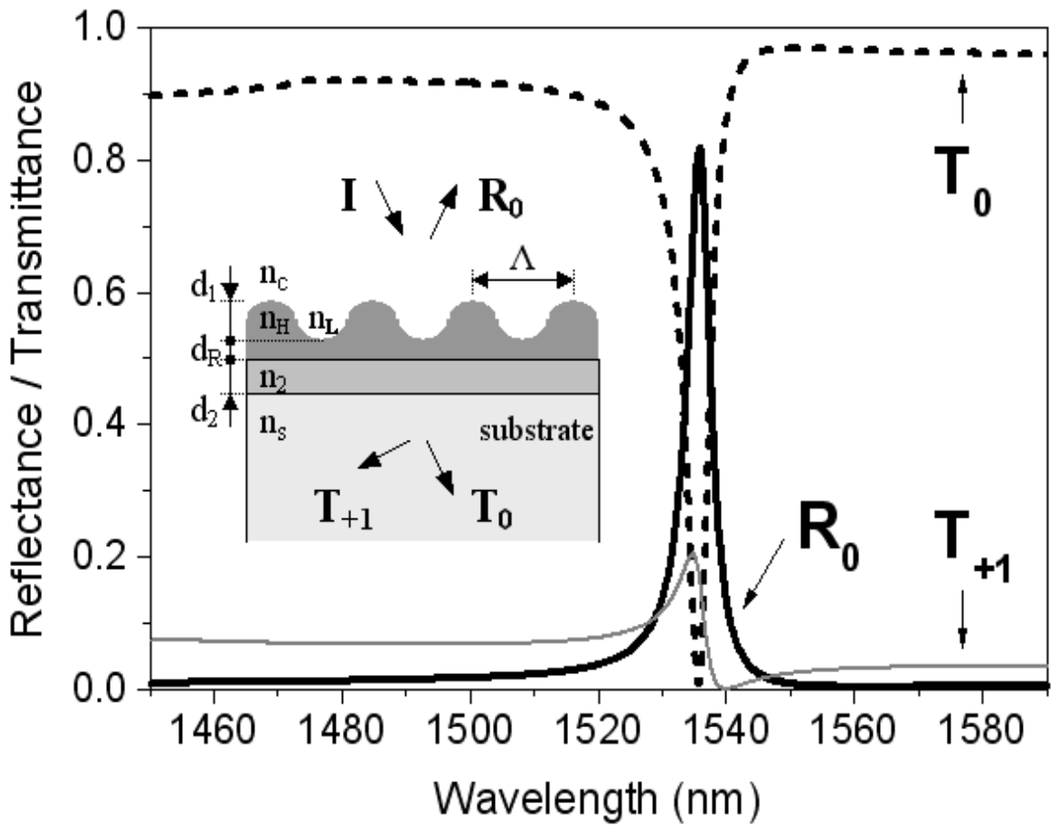

Fig. 11. Calculated spectral filter response with parameters corresponding to those of the fabricated filter for TE polarization. The parameters are as follows: thicknesses, d_1 = 333 nm, d_R = 0 nm (No residue), d_2 = 250 nm; refractive indices n_H = 1.51, n_L = 1.00, n_2 = 1.87, n_c = 1.00, n_s = 1.50; grating period Λ = 1111 nm; incident angle θ_{in} = 10°

Generally, for this device class, there is good agreement between theory and experiment as shown, for example, in (Priambodo et al., 2003) and by the results presented here. As quantified in (Kemme et al., 2003), small variations in the device parameters can shift the location of the resonance peak significantly. A residual layer, shown in the inset in Fig. 11 with thickness d_R, can have significant effects on the spectrum and central filter wavelength. By numerical modeling, the thickness of the residual layer can be estimated. This layer, in this work, is an unwanted layer arising during the soft lithography process. Theoretical calculation shows that the resonance wavelength shifts and the FWHM linewidth decreases as the thickness of the residual layer increases as shown in Fig. 12. By comparing the resonance wavelength and linewidth of the calculated data with the measured data, the thickness of the residual layer is estimated to be ~11 nm.

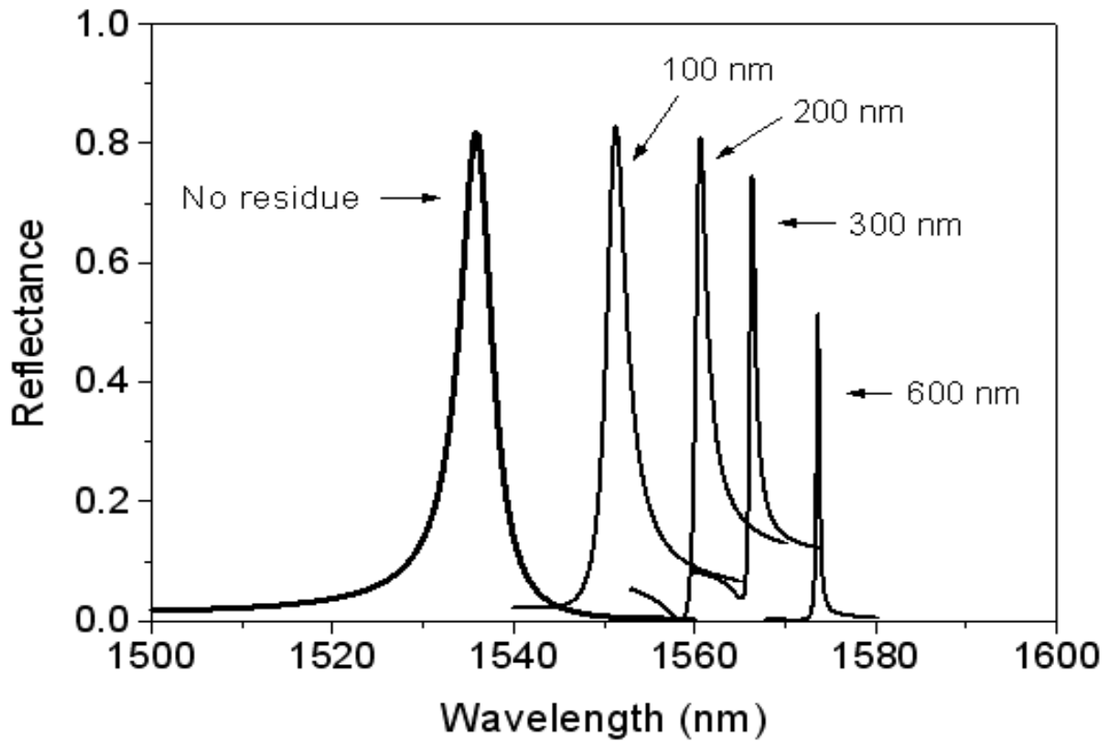

Fig. 12. Calculated spectral response of the fabricated GMR filter with varying thickness of the residual layer (d_R)

Fig. 13 shows a cross-sectional view of the fabricated GMR filter obtained with a scanning electron microscope (SEM, FEI Company, Quanta 3D FEG) indicating no apparent residual layer for the fabricated filter. Moreover, the SEM confirms the parameters used in the theoretical calculations in Fig. 11.

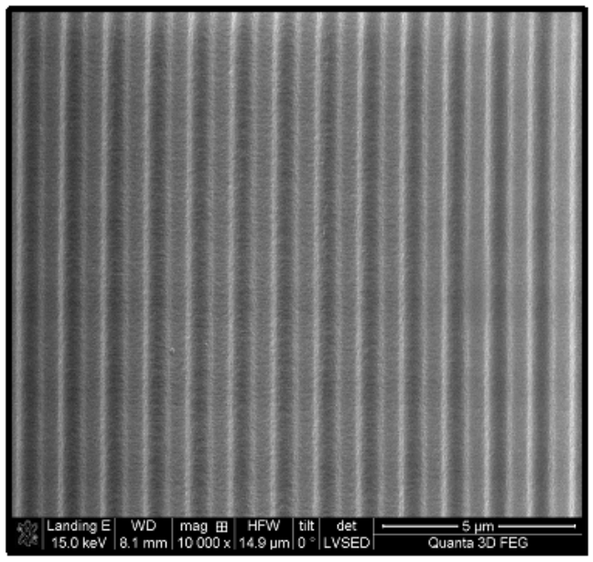

(a)

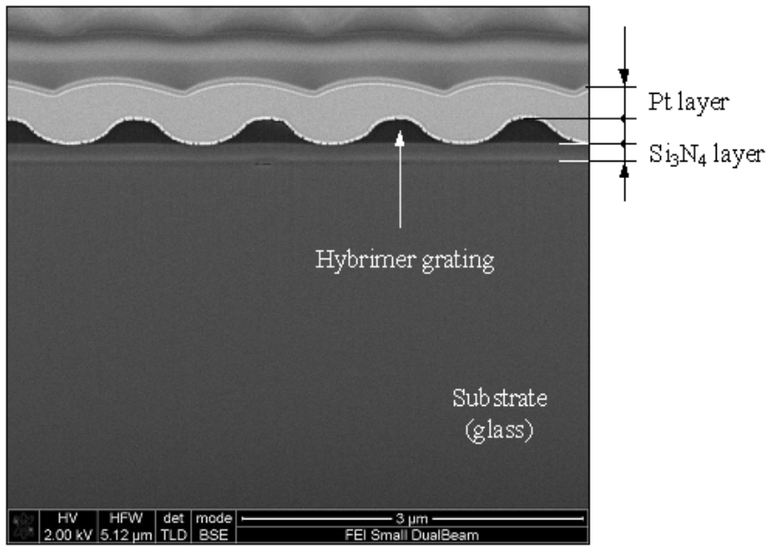

(b)

Fig. 13. SEM images of the fabricated GMR device. (a) Top down view, Magnification = 10,000. The size of the image is ~15 µm. (b) Cross-sectional view, Magnification = 25,000. Note that the white part on top is a platinum (Pt) layer for protection during ion-beam sectioning

4. Conclusion

We presented fabrication and characterization of guided-mode resonant (GMR) filters made by soft lithography. As these resonant elements are highly sensitive to parametric variations, it is important to develop methods for their reliable, repeatable fabrication. Thus, a fabrication process that is consistent and simple, employing an elastomeric mold and a UV-

curable organic-inorganic hybrid material is provided. By combining MIMIC, a hybrimer, and an h-PDMS mold, a photopolymer grating structure is readily fabricated. Measured spectra show ~81% reflectance and ~8% transmittance at a resonance wavelength of 1538 nm. The filter's linewidth is ~4.5 nm, and the sideband reflectance is ~5%. Experimental and theoretical results are in good agreement. The use of hybrimer media yields improved processes and high-quality photonic devices.

5. Acknowledgments

This work was supported in part by the National Science Foundation (NSF) under grant ECCS-0925774 and by the UT System Texas Nanoelectronics Research Superiority Award funded by the State of Texas Emerging Technology Fund. The authors gratefully acknowledge the NanoPort Applications Team at FEI Company for providing the results shown in Fig. 13. The authors thank Prof. B. Huey from The Institute of Materials Science at the University of Connecticut for providing access to AFM facilities. This work was performed in part at the Center for Nanoscale Systems (CNS), a member of the National Nanotechnology Infrastructure Network (NNIN), which is supported by the NSF under award ECS-0335765. CNS is part of the Faculty of Arts and Sciences at Harvard University. Additional support was provided by the Texas Instruments Distinguished University Chair in Nanoelectronics endowment.

6. References

Avrutsky I.A. & Sychugov, V.A. (1989). Reflection of a beam of finite size from a corrugated waveguide. *J. Mod. Opt.*, Vol. 36, No. 11, (1989), pp. 1527-1539, ISSN 1362-3044

Brundrett, D.L.; Gaylord, T.K. & Glytsis, E.N. (1998). Polarizing mirror/absorber for visible wavelengths based on a silicon subwavelength grating: design and fabrication. *Appl. Opt.*, Vol. 37, No. 13, (May 1998), pp. 2534-2541

Choi, D.-G.; Jeong, J.-H.; Sim, Y.-S.; Lee, E.-S.; Kim, W.-S. & Bae, B.-S. (2005). Fluorinated organic-inorganic hybrid mold as a new stamp for nanoimprint and soft lithography. *Langmuir*, Vol. 21, No. 21, (October 2005), pp. 9390-9392

Delamarche, E.; Schmid, H.; Michel, B. & Biebuyck, H. (1997). Stability of molded polydimethylsiloxane microstructures. *Advanced Materials*, Vol. 9, No. 9, (1997), pp. 741-746, ISSN 0935-9648

Ding, Y. & Magnusson, R. Resonant leaky-mode spectral-band engineering and device applications. *Optics Express, V*ol. 12, No. 23, (2004), pp. 5661–5674

Gaylord, T.K. & Moharam, M.G. (1985). Analysis and applications of optical diffraction by gratings. *Proc. IEEE*, Vol. 73, No. 5, (May 1985), pp. 894-937, ISSN 0018-9219

Kemme, S.A.; Peters, D.W.; Wendt, J.R.; Carter, T.R. & Samora, S. Integration and tolerance issues for resonant subwavelength gratings," *Proc. of the SPIE Gradient Index, Miniature, and Diffractive Optical Systems III*, Vol. 5177, pp. 1-8, San Diego, California, USA, August 2003.

Kim, W.-S.; Kim, K.-S.; Eo, Y.-J.; Yoon, K.B. & Bae, B.-S. (2005). Synthesis of fluorinated hybrid material for UV embossing of a large core optical waveguide structure. *J. Mater. Chem.*, Vol. 15, No. 4, (January 2005), pp. 465-469

Kim, W.-S.; Choi, D.-G. & Bae, B.-S. (2006). Ultraviolet-nanoimprint of 40 nm scale patterns using functionally modified fluorinated hybrid materials. *Nanotechnology*, Vol. 17, No. 13, (July 2006), pp. 3319-3324

Lee, D.-H.; Park, K.-H.; Hong, L.-Y. & Kim, D.-P. (2007). SiCN ceramic patterns fabricated by soft lithography techniques. *Sens. Actuators A: Physical*, Vol. 135, No. 2, (April 2007), pp. 895-901

Lee, J.-H.; Kim, C.-H.; Ho, K.-M. & Constant, K. (2005). Two-polymer microtransfer molding for high layered microstructures. *Advanced Materials*, Vol. 17, No. 20, (October 2005), pp. 2481-2485

Lee, K.J.; LaComb, R.; Britton, B.; Shokooh-Saremi, M.; Silva, H.; Donkor, E.; Ding, Y. & Magnusson, R. (2008). Silicon-layer guided-mode resonance polarizer with 40-nm bandwidth. *IEEE Photonics Tech. Lett.*, Vol. 20, No. 22, (November 2008), pp. 1857-1859, ISSN 1041-1135

Lee, K.J. & Magnusson, R. Single-layer resonant high reflector in TE polarization: Theory and experiment. *IEEE Photonics Journal*, Vol. 3, No. 1, (February 2011), pp. 123–129

Lee, T.-H.; Kim, J.H. & Bae, B.-S. (2006). Synthesis of colorless imide hybrid nanocomposites using amine functionalized oligosiloxane nano-building clusters. *J. Mater. Chem.*, Vol. 16, No. 17, (May 2006), pp. 1657-1664

Lee, T.-W.; Mitrofanov, O. & Hsu, J.W.P. (2005). Pattern-transfer fidelity in soft lithography: the role of pattern density and aspect ratio. *Advanced Functional Materials*, Vol. 15, No. 10, (October 2005), pp. 1683-1688

Liu, Z.S.; Tibuleac, S.; Shin, D.; Young, P.P. & Magnusson, R. (1998). High-efficiency guided-mode resonance filter. *Opt. Lett.*, Vol. 23, No. 19, (October 1998), pp. 1556-1558

Magnusson, R. & Wang, S.S. (1992). New principle for optical filters. *Appl. Phys. Lett.*, Vol. 61, No. 9, (August 1992), pp. 1022-1024, ISSN 0003-6951

Norland Products Inc., n.d. Available from: <http://www.norlandprod.com>

Odom, T.W.; Love, J.C.; Wolfe, D.B.; Paul, K.E. & Whitesides, G. W. (2002). Improved pattern transfer in soft lithography using composite stamps. *Langmuir*, Vol. 18, No. 13, (June 2002), pp. 5314-5320

Peng, S. & Morris, G.M. (1996). Experimental demonstration of resonant anomalies in diffraction from two-dimensional gratings. *Opt. Lett.*, Vol. 21, No. 8, (April 1996), pp. 549-551

Priambodo, P.S.; Maldonado, T.A. & Magnusson, R. (2003). Fabrication and characterization of high-quality waveguide-mode resonant optical filters. *Appl. Phys. Lett.*, Vol. 83, No. 16, (October 2003), pp. 3248-3250

Rogers J.A. & Nuzzo, R.G. (2005). Recent progress in soft lithography. *Materials Today*, Vol. 8, No. 2, (February 2005), pp. 50-56

Schmid H. & Michel, B. (2000). Siloxane polymers for high-resolution, high-accuracy soft lithography. *Macromolecules*, Vol. 33, No. 8, (April 2000), pp. 3042-3049

Sharon, A.; Rosenblatt, D. & Friesem, A.A. (1996). Narrow spectral bandwidths with grating waveguide structures. *Appl. Phys. Lett.*, Vol. 69, No. 27, (December 1996), pp. 4154-4156, ISSN 0003-6951

Summers Optical, n.d. Available from: <http://www.optical-cement.com>

Tang, M.D.; Golden, A.P. & Tien, J. (2003). Molding of three-dimensional microstructures of gels. *J. Am. Chem. Soc.*, Vol. 125, No. 43, (October 2003), pp. 12988-12989

Wang, Y.; Flaim, T.; Mercado, R.; Fowler, S.; Holmes, D. & Planje, C. (2005). Hybrid high refractive index polymer coatings, *Proc. of the SPIE Organic Photonic Materials and Devices VII*, Vol. 5724, pp. 42-49, San Jose, California, USA, April 2005

Xia, Y. &Whitesides, G.M. (1998). Soft lithography. *Angewandte Chemie International Edition*, Vol. 37, No. 5, (March 1998), pp. 550-575

Xia, Y.; Rogers, J.A.; Paul, K.E. & Whitesides, G.M. (1999). Unconventional methods for fabricating and patterning nanostructures. *Chem. Rev.*, Vol. 99, No. 7, (July 1999), pp. 1823-1848

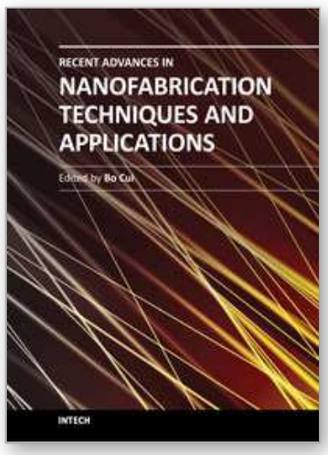

Recent Advances in Nanofabrication Techniques and Applications

Edited by Prof. Bo Cui

ISBN 978-953-307-602-7
Hard cover, 614 pages
Publisher InTech
Published online 02, December, 2011
Published in print edition December, 2011

Nanotechnology has experienced a rapid growth in the past decade, largely owing to the rapid advances in nanofabrication techniques employed to fabricate nano-devices. Nanofabrication can be divided into two categories: "bottom up" approach using chemical synthesis or self assembly, and "top down" approach using nanolithography, thin film deposition and etching techniques. Both topics are covered, though with a focus on the second category. This book contains twenty nine chapters and aims to provide the fundamentals and recent advances of nanofabrication techniques, as well as its device applications. Most chapters focus on in-depth studies of a particular research field, and are thus targeted for researchers, though some chapters focus on the basics of lithographic techniques accessible for upper year undergraduate students. Divided into five parts, this book covers electron beam, focused ion beam, nanoimprint, deep and extreme UV, X-ray, scanning probe, interference, two-photon, and nanosphere lithography.

How to reference

In order to correctly reference this scholarly work, feel free to copy and paste the following:

Kyu J. Lee, Jungho Jin, Byeong-Soo Bae and Robert Magnusson (2011). Guided-Mode Resonance Filters Fabricated with Soft Lithography, Recent Advances in Nanofabrication Techniques and Applications, Prof. Bo Cui (Ed.), ISBN: 978-953-307-602-7, InTech, Available from: http://www.intechopen.com/books/recent-advances-in-nanofabrication-techniques-and-applications/guided-mode-resonance-filters-fabricated-with-soft-lithography

INTECH
open science | open minds

InTech Europe
University Campus STeP Ri
Slavka Krautzeka 83/A
51000 Rijeka, Croatia
Phone: +385 (51) 770 447
Fax: +385 (51) 686 166
www.intechopen.com

InTech China
Unit 405, Office Block, Hotel Equatorial Shanghai
No.65, Yan An Road (West), Shanghai, 200040, China
中国上海市延安西路65号上海国际贵都大饭店办公楼405单元
Phone: +86-21-62489820
Fax: +86-21-62489821

IntechOpen